ChemComm

COMMUNICATION

View Article Online
View Journal | View Issue

Cite this: *Chem. Commun.*, 2023, 59, 9509

Received 13th April 2023,
Accepted 20th June 2023

DOI: 10.1039/d3cc01803b

rsc.li/chemcomm

Combined homogeneous and heterogeneous hydrogenation to yield catalyst-free solutions of parahydrogen-hyperpolarized [1-^{13}C]succinate†‡

James Eills, *[abc] Román Picazo-Frutos,[bc] Dudari B. Burueva,[d] Larisa M. Kovtunova,[de] Marc Azagra,[a] Irene Marco-Rius,[a] Dmitry Budker[bcf] and Igor V. Koptyug *[d]

We show that catalyst-free aqueous solutions of hyperpolarized [1-^{13}C]succinate can be produced using parahydrogen-induced polarization (PHIP) and a combination of homogeneous and heterogeneous catalytic hydrogenation reactions. We generate hyperpolarized [1-^{13}C]fumarate *via* PHIP using para-enriched hydrogen gas with a homogeneous ruthenium catalyst, and subsequently remove the toxic catalyst and reaction side products *via* a purification procedure. Following this, we perform a second hydrogenation reaction using normal hydrogen gas to convert the fumarate into succinate using a solid Pd/Al_2O_3 catalyst. This inexpensive polarization protocol has a turnover time of a few minutes, and represents a major advance for *in vivo* applications of [1-^{13}C]succinate as a hyperpolarized contrast agent.

Hyperpolarization-enhanced magnetic resonance imaging (MRI) and spectroscopy (MRS) allows clinicians to track metabolic processes noninvasively in real time in the body.[1,2] Parahydrogen-induced polarization (PHIP) has emerged as an inexpensive contrast-agent hyperpolarization method.[3–8] Parahydrogen (p-H_2) at >98% para-enrichment can be prepared from normal hydrogen gas (n-H_2) at temperatures below 30 K, and then catalytically reacted with an unsaturated precursor to produce a hyperpolarized product molecule.[9,10] The polarization is transferred to a ^{13}C spin in the molecule,[11–14] and then the hyperpolarized molecule can be injected for *in vivo* imaging,[12,15,16] with more recent work enabling purification prior to injection.[17,18] PHIP relies on hydrogenation reactions, often carried out in an organic solvent using an organometallic catalyst. Since the product must be purified and extracted into an aqueous solution, the number of targets that can be produced in this way is limited. To date only [1-^{13}C]pyruvate and [1-^{13}C]fumarate have been hyperpolarized *via* PHIP and then purified to a sufficient level for safe *in vivo* application.[6,17]

Another promising contrast agent is [1-^{13}C]succinate, which has been used for real-time *in vivo* tumor detection[19] and as a marker for stroke-affected regions of the brain.[20] [1-^{13}C]succinate-d_2 has been produced at high ^{13}C polarization levels *via* PHIP by hydrogenating [1-^{13}C]acetylene dicarboxylate or [1-^{13}C]fumarate-d_2 in aqueous solution,[19,21–25] and studied *in vivo* as a contrast agent,[19,22,23] but in these demonstrations the toxic catalyst remained in the solutions. In an exciting piece of work, [1-^{13}C]maleic anhydride-d_2 was hydrogenated with p-H_2 in $CDCl_3$ to produce [1-^{13}C]succinic anhydride-d_2, which was hydrolyzed with NaOD to yield [1-^{13}C]succinate in the aqueous phase, leaving the catalyst in the organic $CDCl_3$ phase.[26] However, the concentration and polarization of succinate in the aqueous phase were not reported, and the hydrogenation yield was 40%, meaning 60% of the maleic anhydride was likely hydrolyzed to toxic maleate, contaminating the solution.

In contrast to homogeneous catalysis, removal of the catalyst is much easier after a heterogeneous catalytic process since the catalyst and the products represent different phases. Heterogeneous catalysts have been demonstrated to produce PHIP effects.[27,28] However, this approach is generally inferior to homogeneous hydrogenation in terms of achievable polarization levels (often 1–3% or even less) since the p-H_2-derived atoms can migrate across the catalyst surface and lose their correlated spin state (and hence polarization). Hydrogen atom mobility can be suppressed by poisoning the catalyst surface,[29] or by moving to supported-metal catalysts with smaller active sites[27,30] or even single-atom solid catalysts,[31,32] but this comes at the cost of catalytic activity.

In this work we leverage the advantages of both homogeneous and heterogeneous catalysis to produce hyperpolarized [1-^{13}C]-succinate. We employ an established method to hyperpolarize [1-^{13}C]fumarate *via* homogeneous PHIP, yielding the pure molecule

[a] *Institute for Bioengineering of Catalonia, Barcelona Institute of Science and Technology, Barcelona 08028, Spain. E-mail: jeills@ibecbarcelona.eu*
[b] *Helmholtz-Institut Mainz, GSI Helmholtzzentrum für Schwerionenforschung, Mainz 55128, Germany*
[c] *Institute for Physics, Johannes Gutenberg-Universität Mainz, Mainz 55099, Germany*
[d] *International Tomography Center SB RAS, Novosibirsk 630090, Russia. E-mail: koptyug@tomo.nsc.ru*
[e] *Boreskov Institute of Catalysis SB RAS, Novosibirsk 630090, Russia*
[f] *Department of Physics, University of California, Berkeley, CA 94720-7300, USA*

† This manuscript is based on work done prior to February 24, 2022.

‡ Electronic supplementary information (ESI) available. See DOI: https://doi.org/10.1039/d3cc01803b

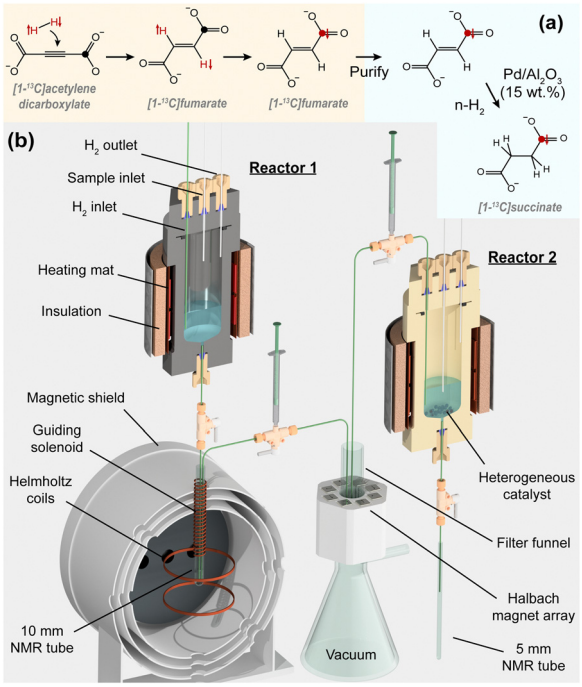

Fig. 1 (a) The formation of hyperpolarized [1-^{13}C]fumarate in Reactor 1, purification, and subsequent hydrogenation to [1-^{13}C]succinate. (b) The apparatus used for the succinate hyperpolarization procedure described in the main text.

Table 1 Summary of fumarate → succinate hydrogenation experiments under different conditions

Catalyst	Loading (mg)	T (°C)	H_2 flow rate (mL min^{-1})	Yield (%)
Pt/Al_2O_3	20	90	80	32
Pd/C	20	90	80	66
Pd/Al_2O_3	20	90	80	70
	20	90	120	85
	30	98	150	98

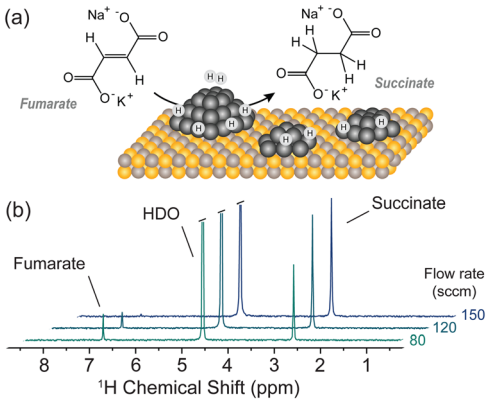

Fig. 2 (a) The heterogeneously-catalyzed hydrogenation of fumarate to succinate. Yellow and grey balls represent alumina and black balls represent palladium. (b) ^{1}H NMR spectra of three reaction solutions after bubbling H_2 through 100 mM disodium fumarate in D_2O over 20 wt% Pd/Al_2O_3. These three spectra correspond to the last three rows of Table 1.

in an aqueous solution at >20% ^{13}C polarization.[6] From this point, a heterogeneous hydrogenation catalyst is used to facilitate a second hydrogenation step using n-H_2 to produce hyperpolarized [1-^{13}C]succinate, and the ^{13}C polarization survives this process. The concept and the experimental apparatus are shown in Fig. 1.

For the hydrogenation of fumarate to succinate, we tested different heterogeneous catalysts. 20–30 mg of catalyst was loaded into a pressurizable 5 mm NMR tube containing 500 μL of 100 mM sodium fumarate in D_2O, and the sample was heated. Hydrogen gas (not para-enriched) was then bubbled through the solution at 6 bar to initiate the reaction. After 30 s, the tube was depressurized and the solution was extracted from the NMR tube and filtered to remove the catalyst. ^{1}H NMR spectra were acquired from the samples in a 7.05 T magnet. The experiments and results are summarized in Table 1.

From the ^{1}H NMR spectra we were able to quantify the fumarate and succinate concentrations, and hence determine the reaction yield. Pd/Al_2O_3 performed best and was selected for following experiments due to good powder properties (wettability, flowability, and chemical stability). The ^{1}H NMR spectra for the three reactions using Pd/Al_2O_3 are shown in Fig. 2. From these spectra we were unable to detect any reaction side-products (*e.g.*, the *cis*-isomer maleate, or hydrogenolysis products from C–C or C–O bond scission), indicating excellent reaction selectivity. For all subsequent experiments, we used (unless otherwise specified) 15 wt% Pd supported on Al_2O_3 as the heterogeneous catalyst. See ESI‡ for the catalyst characterization data.

To quantify the residual Pd content in the succinate solution after the heterogeneous hydrogenation, the experiment from the last line of Table 1 was repeated twice (500 μL of 100 mM sodium fumarate containing 30 mg 15 wt% Pd/Al_2O_3 at 98, H_2 bubbling for 30 s at 6 bar). Immediately following the reaction, the sample was syringe-filtered (0.2 μm pore diameter, Chromafil Xtra H-PTFE-20/25) in <3 s to remove the heterogeneous catalyst. ICP-MS (inductively-coupled plasma mass spectrometry) analysis was then carried out on these two samples. No Pd was observed, meaning the concentration in the solution was <5 μM, corresponding to the ICP-MS detection sensitivity (after solution dilution). See ESI‡ for further details.

Hydrogenation of acetylene dicarboxylate was carried out using parahydrogen (>98% para-enrichment) and a homogeneous catalyst ($[RuCp^*(MeCN)_3]PF_6$) in D_2O to produce fumarate with the protons in a hyperpolarized state. 2.2% of the fumarate molecules are the naturally-occurring [1-^{13}C] isotopologue, and a magnetic field cycle[33] was applied to the sample to transfer the proton hyperpolarization to the ^{13}C nucleus in those molecules. 200–250 μL of this solution was taken (sample A) and placed in a 1.4 T benchtop NMR magnet for ^{13}C signal acquisition. The average [1-^{13}C]fumarate concentration in this sample was 43 ± 5 mM, and the ^{13}C polarization was 23 ± 2%. The remainder of the hyperpolarized fumarate sample underwent a purification procedure: we mixed the hyperpolarized fumarate solution with 370 ± 20 μL of a 1 M disodium fumarate in D_2O solution (to raise the overall fumarate concentration in order to speed up the precipitation step), and HCl was added to the sample to induce precipitation of solid fumaric acid. The remaining reaction solution was vacuum-filtered off. The fumaric acid was redissolved in 1 mL of 1 M NaOD in D_2O (unless otherwise specified) to yield a clean aqueous solution of ^{13}C-polarized [1-^{13}C]fumarate (sample B).

Sample B was injected into a second hydrogenation reactor (Reactor 2) held at 85 °C, pre-loaded with 15 wt% Pd/Al_2O_3 powder. Hydrogen gas was bubbled through the mixture at 6 L min^{-1} and a pressure of 8.5 bar for 20 s. A two-way valve was opened to release the solution into a 5 mm NMR tube beneath Reactor 2, and the solid catalyst was caught in a 1/8 in. capillary directly above two-way valve (because the valve inner diameter was smaller than the catalyst pellets), yielding clean aqueous succinate solutions. The 5 mm NMR tube containing sample B was placed in the 1.4 T benchtop NMR magnet for signal acquisition. The experimental apparatus is shown in Fig. 1, and experimental details are provided in the ESI.‡

The complete procedure described above was repeated six times with different amounts of Pd/Al_2O_3 present. The [1-^{13}C]fumarate and [1-^{13}C]succinate polarizations and reaction yields are shown in Fig. 3(a). The average concentration of fumarate in the sample prior to the fumarate → succinate hydrogenation was 180 ± 40 mM. The polarizations reported are those of the molecules in solution that underwent the hyperpolarization process, discounting the unpolarized molecules added during the purification process (see ESI‡). Reactor 2 was not cleaned between experiments, meaning there was residual heterogeneous catalyst left after each run: note that in Run 5 no new heterogeneous catalyst was added to the reactor, but the reaction yield was still 8.0%.

The procedure was repeated another four times to investigate the effect of solution pH. The solution used to redissolve the purified fumaric acid was at 0.5 M NaOD concentration for the first two runs, and 0.2 M NaOD concentration for the next two, yielding reaction solutions with pH 14 and pH 3, respectively. The results are shown in Fig. 3(b). The ^{13}C polarization of both [1-^{13}C]fumarate and [1-^{13}C]succinate is an order of magnitude lower when the reaction solution is acidic. The reason for this is subject to ongoing investigation.

An experiment was carried out as described before, but with 22% ^{13}C enrichment in the C1 position of the acetylene dicarboxylate. The resulting ^{13}C NMR spectrum of the hyperpolarized reaction solution is shown in Fig. 3(c) alongside a thermal-equilibrium ^{13}C spectrum of a 500 mM ^{13}C-labelled standard, also acquired at 1.4 T. The ^{13}C polarization of the hyperpolarized [1-^{13}C]succinate molecules was measured to be 11.9%. The polarization is higher than the results in Fig. 3(a) because the sample purification and transport steps were faster. The ^{13}C T_1 times of [1-^{13}C]fumarate and [1-^{13}C]succinate in the purified aqueous solution (D_2O, pH 14) were measured at 1.4 T by pulsing every 7.2 s with a 5° flip-angle pulse. The results are plotted in Fig. 3(d).

Our results show that this two-step hydrogenation is a viable method for the production of hyperpolarized [1-^{13}C]succinate for biological applications. The [1-^{13}C]succinate ^{13}C polarization is consistently lower than that of [1-^{13}C]fumarate, likely due to a relaxation process. This may be a catalyst-surface effect, or a solution-state T_1 difference at the lower fields experienced during hydrogenation and sample transport.

For the fumarate purification we mixed the hyperpolarized fumarate solution with a solution of 1 M unpolarized fumarate

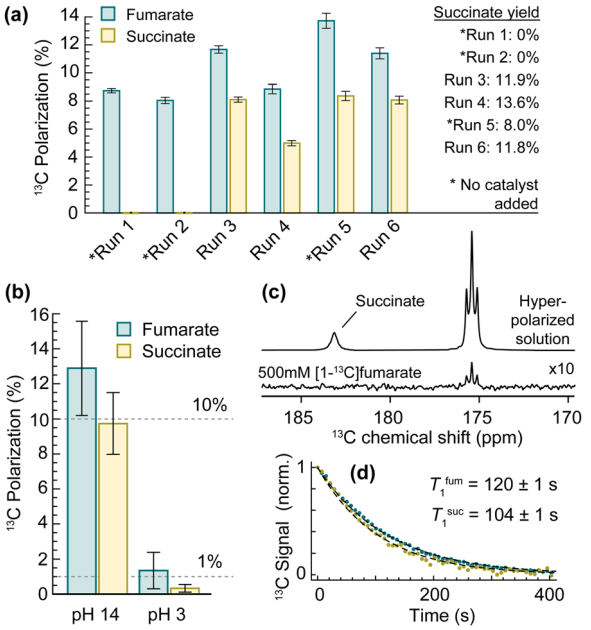

Fig. 3 (a) ^{13}C polarization of [1-^{13}C]fumarate and [1-^{13}C]succinate for a series of experiments. The mass of heterogeneous catalyst added to Reactor 2 was 0, 0, 47, 62, 0, 52 mg for Runs 1 to 6, and the reactor was not cleaned between experiments. The error bars indicate uncertainty of the sample volumes used (see ESI‡). (b) ^{13}C polarizations for experiments in which the fumarate → succinate hydrogenation was carried out at different pH. Two replicates were performed for each pH, and the error bars represent the standard errors. (c) A comparison between ^{13}C NMR spectra of a hyperpolarized reaction solution at 22% ^{13}C-labelling of the fumarate and succinate, and a 500 mM thermal-equilibrium standard of 100% ^{13}C-labelled [1-^{13}C]fumarate. The hyperpolarized spectrum was acquired with a 30° flip-angle pulse, and the thermal-equilibrium spectrum was acquired with a 90° pulse. The succinate ^{13}C polarization (accounting for the excitation pulse flip-angle difference) was 11.9% and the succinate yield was 16.8%. (d) Relaxation of the hyperpolarized fumarate (teal) and succinate (yellow) ^{13}C signals at 1.4 T.

to raise the overall concentration to speed up the precipitation step. This is not necessary if higher hydrogen gas pressure and starting material concentration are used, to form fumarate in ~ 200 mM or higher concentration to allow direct precipitation from the reaction solution.[34]

In high resolution ^{1}H NMR spectra we observed that the succinate formed was partially deuterated during the heterogeneous hydrogenation (by D atoms from D_2O mixing with H atoms on the surface of the heterogeneous catalyst). We carried out six additional 30 s hydrogenation experiments at 98 °C using 10, 15, and 20 wt% Pd/Al_2O_3, and observed on average 16.5 ± 1.5% deuteration of the succinate: 43% succinate-h_4, 50% succinate-d_1 and 8% succinate-2,3-d_2. This would lead to underestimating the succinate concentration with ^{1}H NMR, so we corrected for this factor in all results (including in Table 1).

The fumarate → succinate yield in Reactor 2 was consistently lower than in experiments carried out in a 5 mm NMR tube. We believe this is because in the reactor the catalyst particles were not well-agitated during hydrogen bubbling. Higher succinate yields should be readily achievable by optimizing the reaction vessel.

We have demonstrated a novel, inexpensive method to produce catalyst-free hyperpolarized succinate solutions *via* PHIP. We

achieve 11.9% ^{13}C polarization in [1-^{13}C]succinate, which is high-enough for *in vivo* applications. The heterogeneous catalyst employed (Pd/Al_2O_3) showed 100% selectivity for fumarate → succinate conversion, and we do not detect side products or contaminants in the succinate solutions. There are a few aspects that make this approach particularly promising: (1) heterogeneously hydrogenating *prepolarized* fumarate makes the relatively low PHIP efficiency of heterogeneous catalysts irrelevant; (2) The heterogeneous hydrogenation is highly efficient, with a reaction yield of $>98\%$ in 30 s (Table 1 and Fig. 2); (3) Most of the fumarate ^{13}C polarization survives the heterogeneous hydrogenation step; (4) The heterogeneous hydrogenation does not produce side products within our measurement sensitivity, so the final solutions appear to be biocompatible; (5) After syringe-filtering the succinate solution, we were unable to detect residual Pd metal, meaning the concentration was less than the ICP-MS measurement sensitivity of 5 μM. In a 1 mL solution this would correspond to $\lesssim 0.5$ μg, far below the LD50 values of Pd complexes which are often on the order of milligrams kg^{-1}.[35] We believe this work marks an exciting new class of hyperpolarization experiments in which a rapid chemical synthesis/modification is carried out on a purified hyperpolarized molecule to produce a specific target.

This project has received funding from the European Union's Horizon 2020 Research and Innovation Programme under the Marie Sklodowska-Curie Grant Agreements 766402 and 101063517, the DFG (Project ID 465084791), from the Spanish Ministry under projects MCIN/AEI/10.13039/501100011033 (Ref. PID2020-117859RA-I00 and RYC2020-029099-I), by "ESF Investing in your future", the European Union's Horizon 2020 research and innovation program (GA-863037), and the BIST – "la Caixa" initiative in Chemical Biology (CHEMBIO). I. V. K. and D. B. B. thank the Russian Science Foundation (Grant #22-43-04426) for financial support.

Conflicts of interest

There are no conflicts to declare.

References

1 J. Eills, D. Budker, S. Cavagnero, E. Y. Chekmenev, S. J. Elliott, S. Jannin, A. Lesage, J. Matysik, T. Meersmann, T. Prisner, J. A. Reimer, H. Yang and I. V. Koptyug, *Chem. Rev.*, 2023, **123**, 1417–1551.
2 S. J. Nelson, J. Kurhanewicz, D. B. Vigneron, P. E. Larson, A. L. Harzstark, M. Ferrone, M. Van Criekinge, J. W. Chang, R. Bok and I. Park, *et al.*, *Sci. Transl. Med.*, 2013, **5**, 198ra108–198ra108.
3 J.-B. Hövener, A. N. Pravdivtsev, B. Kidd, C. R. Bowers, S. Glöggler, K. V. Kovtunov, M. Plaumann, R. Katz-Brull, K. Buckenmaier and A. Jerschow, *et al.*, *Angew. Chem., Int. Ed.*, 2018, **57**, 11140–11162.
4 S. Korchak, M. Emondts, S. Mamone, B. Blümich and S. Glöggler, *Phys. Chem. Chem. Phys.*, 2019, **21**, 22849–22856.
5 J. Eills, E. Cavallari, C. Carrera, D. Budker, S. Aime and F. Reineri, *J. Am. Chem. Soc.*, 2019, **141**, 20209–20214.
6 S. Knecht, J. W. Blanchard, D. Barskiy, E. Cavallari, L. Dagys, E. Van Dyke, M. Tsukanov, B. Bliemel, K. Münnemann and S. Aime, *et al.*, *Proc. Natl. Acad. Sci. U. S. A.*, 2021, **118**, e2025383118.
7 W. G. Hale, T. Y. Zhao, D. Choi, M.-J. Ferrer, B. Song, H. Zhao, H. E. Hagelin-Weaver and C. R. Bowers, *Chem. Phys. Chem.*, 2021, **22**, 822–827.
8 S. Mamone, A. P. Jagtap, S. Korchak, Y. Ding, S. Sternkopf and S. Glöggler, *Angew. Chem., Int. Ed.*, 2022, **61**, e202206298.
9 C. R. Bowers and D. P. Weitekamp, *J. Am. Chem. Soc.*, 1987, **109**, 5541–5542.
10 A. B. Schmidt, C. R. Bowers, K. Buckenmaier, E. Y. Chekmenev, H. de Maissin, J. Eills, F. Ellermann, S. Glöggler, J. W. Gordon and S. Knecht, *et al.*, *Anal. Chem.*, 2022, **94**, 479–502.
11 M. Goldman and H. Jóhannesson, *C. R. Phys.*, 2005, **6**, 575–581.
12 M. Goldman, H. Jóhannesson, O. Axelsson and M. Karlsson, *Magn. Reson. Imaging*, 2005, **23**, 153–157.
13 J. Eills, G. Stevanato, C. Bengs, S. Glöggler, S. J. Elliott, J. Alonso-Valdesueiro, G. Pileio and M. H. Levitt, *J. Magn. Reson.*, 2017, **274**, 163–172.
14 M. Emondts, J. F. P. Colell, B. Blümich and P. P. M. Schleker, *Phys. Chem. Chem. Phys.*, 2017, **19**, 21933–21937.
15 P. Bhattacharya, E. Y. Chekmenev, W. F. Reynolds, S. Wagner, N. Zacharias, H. R. Chan, R. Bünger and B. D. Ross, *NMR Biomed.*, 2011, **24**, 1023–1028.
16 A. B. Schmidt, S. Berner, M. Braig, M. Zimmermann, J. Hennig, D. von Elverfeldt and J.-B. Hövener, *PLoS One*, 2018, **13**, 1–15.
17 E. Cavallari, C. Carrera, M. Sorge, G. Bonne, A. Muchir, S. Aime and F. Reineri, *Sci. Rep.*, 2018, **8**, 8366.
18 N. J. Stewart, H. Nakano, S. Sugai, M. Tomohiro, Y. Kase, Y. Uchio, T. Yamaguchi, Y. Matsuo, T. Naganuma and N. Takeda, *et al.*, *Chem. Phys. Chem.*, 2021, **22**, 915–923.
19 N. M. Zacharias, C. R. McCullough, S. Wagner, N. Sailasuta, H. R. Chan, Y. Lee, J. Hu, W. H. Perman, C. Henneberg and B. D. Ross, *et al.*, *J. Mol. Imaging Dyn.*, 2016, **6**, 1000123.
20 B. Ross, P. Bhattacharya, S. Wagner, T. Tran and N. Sailasuta, *Am. J. Neuroradiol.*, 2010, **31**, 24–33.
21 E. Y. Chekmenev, J. Hövener, V. A. Norton, K. Harris, L. S. Batchelder, P. Bhattacharya, B. D. Ross and D. P. Weitekamp, *J. Am. Chem. Soc.*, 2008, **130**, 4212–4213.
22 P. Bhattacharya, E. Y. Chekmenev, W. H. Perman, K. C. Harris, A. P. Lin, V. A. Norton, C. T. Tan, B. D. Ross and D. P. Weitekamp, *J. Magn. Reson.*, 2007, **186**, 150–155.
23 N. M. Zacharias, H. R. Chan, N. Sailasuta, B. D. Ross and P. Bhattacharya, *J. Am. Chem. Soc.*, 2012, **134**, 934–943.
24 S. Berner, A. B. Schmidt, F. Ellermann, S. Korchak, E. Y. Chekmenev, S. Glöggler, D. von Elverfeldt, J. Hennig and J.-B. Hövener, *Phys. Chem. Chem. Phys.*, 2021, **23**, 2320–2330.
25 L. Dagys, C. Bengs, G. A. I. Moustafa and M. H. Levitt, *Chem. Phys. Chem.*, 2022, **23**, e202200274.
26 F. Reineri, A. Viale, S. Ellena, T. Boi, V. Daniele, R. Gobetto and S. Aime, *Angew. Chem., Int. Ed.*, 2011, **50**, 7350–7353.
27 K. Kovtunov, I. Beck, V. Bukhtiyarov and I. Koptyug, *Angew. Chem., Int. Ed.*, 2008, **47**, 1492–1495.
28 K. V. Kovtunov, O. G. Salnikov, I. V. Skovpin, N. V. Chukanov, D. B. Burueva and I. V. Koptyug, *Pure Appl. Chem.*, 2020, **92**, 1029–1046.
29 S. Glöggler, A. M. Grunfeld, Y. N. Ertas, J. McCormick, S. Wagner, P. P. M. Schleker and L.-S. Bouchard, *Angew. Chem., Int. Ed.*, 2015, **54**, 2452–2456.
30 V. V. Zhivonitko, K. V. Kovtunov, I. E. Beck, A. B. Ayupov, V. I. Bukhtiyarov and I. V. Koptyug, *J. Phys. Chem. C*, 2011, **115**, 13386–13391.
31 A. Corma, O. G. Salnikov, D. A. Barskiy, K. V. Kovtunov and I. V. Koptyug, *Chem. – Eur. J.*, 2015, **21**, 7012–7015.
32 I. V. Skovpin, L. M. Kovtunova, A. V. Nartova, R. I. Kvon, V. I. Bukhtiyarov and I. V. Koptyug, *Catal. Sci. Technol.*, 2022, **12**, 3247–3253.
33 B. A. Rodin, J. Eills, R. Picazo-Frutos, K. F. Sheberstov, D. Budker and K. L. Ivanov, *Phys. Chem. Chem. Phys.*, 2021, **23**, 7125–7134.
34 M. Gierse, L. Nagel, M. Keim, S. Lucas, T. Speidel, T. Lobmeyer, G. Winter, F. Josten, S. Karaali and M. Fellermann, *et al.*, *J. Am. Chem. Soc.*, 2023, **145**, 5960–5969.
35 S. Czerczak, J. P. Gromiec, A. Pałaszewska-Tkacz and A. Świdwińska-Gajewska, *Pattys Toxicology*, John Wiley and Sons Ltd, New York, 6th edn, 2012, pp. 653–768.

